ADVANCED TURBULENCE MODELLING OF THE FLOW IN A GENERIC WING-BODY JUNCTION

Michael A. Leschziner
Aeronautics Department
Imperial College of Science, Technology and Medicine, Prince Consort Rd., London SW7 2BY
mike.leschziner@ic.ac.uk

David D. Apsley
Department of Civil and Construction Engineering
UMIST, Manchester M60 1QD
d.apsley@umist.ac.uk

ABSTRACT

The predictive performance of several turbulence models, among them formulations based on non-linear stress-strain relationships and on stress-transport equations, is examined for a spanwise-symmetric 3D flow around a generic wing-body junction, consisting of a modified form of a NACA 0020 aerofoil mounted on a flat plate. The dominant flow feature is a pronounced horseshoe vortex evolving in the junction region following separation and recirculation ahead of the aerofoil's leading edge. This case is one of 6 forming a broad collaborative university-industry programme of turbulence-model investigation. In total, 12 turbulence models have been studied, of which 4 representative forms are considered in this paper. Model performance is judged on the basis of solutions for the velocity and Reynolds-stress fields in the vortical flow upstream of the wing nose and across a downstream cross-flow plane. The emphasis of the study is on the structure of the horseshoe vortex and its effects on the forward flow. The main finding of the study is that, for this particular 3D flow, second-moment closure offers clear predictive advantages over the other models examined.

1 INTRODUCTION

The interaction of a boundary layer with a wall-mounted obstacle partially blocking the flow is a generic process encountered in numerous fluid-flow situations, among them wing-body junctions, blade-hub assemblies in turbomachines, bridge pillars in rivers, buildings subjected to wind and fins or fences mounted on plates to energise the boundary layer or increase heat transfer. The flow is characterised by the formation of a horse-shoe vortex around the obstacle, which induces strong streamwise vorticity and can have a profound effect on the structure of the flow in the vicinity of the wall/obstacle junction. The vortex is initiated at the forward stagnation region at which a recirculation zone is provoked close to the obstacle's base, and this is often observed to contain several weak, unsteady (bimodal) secondary eddies (Baker, 1985; Devenport and Simpson, 1990). As the forward flow realigns the vorticity in the direction of the flow, a strong transverse circulation is set up in the junction, and the flow becomes highly three-dimensional. One important practical consequence of the secondary motion is the transverse convection of streamwise momentum which energises the low-momentum flow in the corner of the junction, thus counteracting any tendency towards separation which may be induced by an adverse pressure gradient.

Junction flows possess particular features which are pertinent to the question of what modelling strategy is likely to be effective. First, the combination of strong curvature, swirl and normal straining in the stagnation region suggests that the anisotropy of the turbulent normal stresses and its interaction with the various strain components are likely to be influential and need to be modelled realistically. Such realism is offered, principally, by second-moment closure. Second, much of the important action takes place close to the wall, especially in the upstream stagnation corner, and this leads to the expectation that the structure of the semi-viscous near-wall region needs to be resolved in detail. This requirement is reinforced by the strong flow skewness close to the wall, caused by the transverse motion that is associated with the horseshoe vortex. A particularly difficult modelling task is to represent correctly the streamwise evolution of the vortex, especially if this has to be done over long distances. This evolution is dictated, principally, by interaction between the shear stress components and curvature within the swirling vortex.

An indication of the complexity of turbulence field in a wing-body junction flow is given by Shabaka and Bradshaw's (1981) analysis of their own measurements which revealed that the eddy viscosities associated with linear stress-strain relationships applied to the shear stresses are highly anisotropic and negative over a significant portion of the flow. This observation, on its own, suggests that a realistic description of the turbulence fields

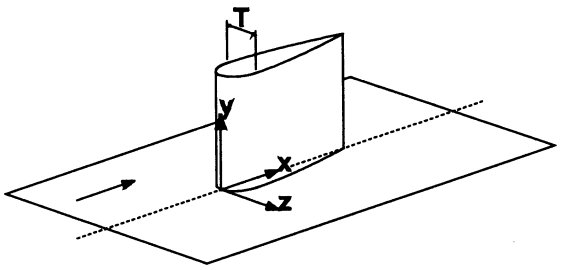

Figure 1: Test-case geometry.

requires the use of second-moment closure, or at least models which are based on non-linear stress-strain relations. An added fundamental difficulty is that the unsteady nature of the recirculating flow at the upstream stagnation zone militates against the use of any statistical turbulence model as a means of resolving properly this type of flow.

The present paper addresses the question of what class of statistical model, if any, is able to return an acceptable predictive performance for the flow around a wing-body junction – a question previously considered in various ways by Chen (1995), Parneix *et al* (1998), Fu *et al* (1997) and Rodi *et al* (1995). The particular geometry studied, Figure 1, is a 3:2 semi-elliptic nose connected to a NACA 0020 tail, for which detailed experimental data have been obtained by Devenport and Simpson (1990) and Fleming *et al* (1993). This flow is one of six cases examined within a broad, tightly-coordinated and interactive turbulence-model investigation involving six partners: UMIST, Loughborough University (LUT), BAE Systems, DERA, ARA and Rolls Royce Aeroengines. Its overall objective was to identify best modelling practices for flows involving separation, stagnation, strong three-dimensional straining and shock/boundary-layer interaction. The collaboration involved the use of several computational procedures and a range of turbulence models, including non-linear-eddy-viscosity and second-moment closure formulations, for prescribed boundary conditions and meshes. This interactive approach is in contrast to earlier investigations, notably that associated with the ERCOFTAC Workshop at the University of Karlsruhe in 1995 (Rodi *et al*, 1995), thus giving increased confidence that the present computational solutions provide a reliable statement on the predictive performance of the turbulence models being examined.

2 TURBULENCE MODELLING

Against the background of the modelling challenges outlined in the introduction, one major objective of the collaborative study was to investigate the benefits of moving away from linear eddy-viscosity models, of whatever ilk, to non-linear models and second-moment closure. The range of models examined and partners contributing related solutions are given in Table 1. Of these, only four models are examined in detail in the computational results to follow – namely, the Launder-Sharma k-ε model, the SST model, the non-linear EVM of Lien *et al* and the low-Re RSTM of Jakirlic and Hanjalic. Linear eddy-viscosity models served, principally, as a datum against which to compare more elaborate practices.

Model	Reference	Computed
High-Re k-ε	Launder & Spalding (1974)	UMIST, LUT
Low Re k-ε	Launder & Sharma (1974)	UMIST, ARA
	Lien & Leschziner (1993)	UMIST
k-ω	Wilcox (1988a)	UMIST
SST k-ω	Menter (1994)	UMIST, ARA
k-g ($g \equiv \omega^{-1/2}$)	Kalitzin *et al* (1996)	BAE
Cubic k-ε EVM	Lien *et al* (1996)	UMIST
	Apsley & Leschziner (1998)	UMIST
High-Re RSTM(ε)	Gibson & Launder (1978)	UMIST
	Speziale *et al* (1991)	UMIST
Low-Re RSTM(ε)	Jakirlic & Hanjalic (1995)	UMIST
Multi-scale RSTM(ω)	Wilcox (1988b)	ARA, UMIST

Table 1: Turbulence models examined.

Cubic eddy-viscosity models may be written, collectively, as follows:

$$\begin{aligned}\mathbf{a} &= -2f_\mu C_\mu \mathbf{s} \\ &+\beta_1\left(\mathbf{s}^2 - \tfrac{1}{3}s_2\mathbf{I}\right)+\beta_2(\mathbf{ws}-\mathbf{sw})+\beta_3\left(\mathbf{w}^2 - \tfrac{1}{3}w_2\mathbf{I}\right) \\ &-\gamma_1 s_2\mathbf{s}-\gamma_2 w_2\mathbf{s}-\gamma_3(\mathbf{w}^2\mathbf{s}+\mathbf{sw}^2 - w_2\mathbf{s}-\tfrac{2}{3}\{\mathbf{wsw}\}\mathbf{I}) \\ &-\gamma_4\left(\mathbf{ws}^2-\mathbf{s}^2\mathbf{w}\right) \qquad (1)\end{aligned}$$

where, for any second-rank tensor $\mathbf{T} = (T_{ij})$,

$$\{\mathbf{T}\} \equiv trace(\mathbf{T}),\quad T_n \equiv \{\mathbf{T}^n\},\quad \mathbf{I} \equiv (\delta_{ij}) \qquad (2)$$

and the *dimensionless* tensors - anisotropy $\mathbf{a}$, mean strain $\mathbf{s}$ and mean vorticity $\mathbf{w}$ - are defined by:

$$a_{ij} = \frac{\overline{u_i u_j}}{k} - \frac{2}{3}\delta_{ij},$$

$$s_{ij} = \tfrac{1}{2}(U_{i,j}+U_{j,i})\frac{1}{\tau},\quad w_{ij} = \tfrac{1}{2}(U_{i,j}-U_{j,i})\frac{1}{\tau} \qquad (3)$$

where τ is the time scale of turbulence, here derived from k and ε, but also determinable from any other length-scale parameter (e.g. ω or g). The particular model for which results are presented below (Lien *et al*, 1996) combines, in essence, the quadratic model of Shih *et al* (1995) with a cubic fragment of the form used by Craft *et al* (1996).

It may be readily demonstrated (eg. Apsley *et al*, 1998) that the quadratic terms in (1) allow anisotropy to be represented, while the cubic terms provide a means for sensitising the stresses to the

stabilising as well as destabilising effects of curvature strain and swirl.

Second-moment closure entails the solution of transport equations for all six components of the Reynolds stresses. On the assumption that stress diffusion is approximated by a "General Gradient Diffusion Hypothesis", the stress-transport equations may be written,

$$\frac{D}{Dt}\overline{u_i u_j} = \frac{\partial}{\partial x_k}(c_s \overline{u_l u_k} \frac{k}{\varepsilon} \frac{\partial \overline{u_i u_j}}{\partial x_l}) + P_{ij} + \Phi_{ij} - \varepsilon_{ij} \quad (4)$$

The representative variant examined below is the low-Re model of Jakirlic and Hanjalic (1995), in which the pressure-strain process is represented by linear approximations which are, essentially, modified forms of those used in the high-Re model of Gibson and Launder (1978). The modifications include a sensitisation of the pressure-strain process to invariants of the stress and dissipation anisotropies and the turbulent Reynolds number. The above, combined with an algebraic approximation for the anisotropic dissipation and near-wall-related modifications to the dissipation-rate equation, are designed to ensure that the wall-asymptotic variation of the Reynolds stresses is returned correctly. A further second-moment closure featuring in one inter-partner comparison to follow is the "multi-scale" model of Wilcox (1988b). This considers the turbulence energy as divided into two spectral partitions. The model therefore includes one extra transport equation for the upper-partition energy.

3 NUMERICAL ISSUES

While the various contributions to the comparisons presented later arose from different numerical procedures, all adopted second-order spatial discretisation practices. The schemes of Loughborough and UMIST are both based on a SIMPLE-type pressure-correction algorithm. Advection in UMIST's procedure is approximated by a TVD form of the quadratic QUICK scheme, while Loughborough's approximation is unbounded. In contrast, ARA's procedure combines a cell-vertex storage arrangement with central differencing in space and 4th-order Runge-Kutta time-marching.

Careful attention was paid to the question of grid-dependence, and a number of preliminary calculations were undertaken to determine the grid that needed to be employed to secure essentially grid-independent results. A particular aspect of these studies was an investigation of the effects of selective refinement in different zones, with special emphasis being placed on the near-nose region. These studies led to the adoption of two grids, both being single-block C-meshes: a 144x48x48-control volume grid for low-*Re* models and a 144x36x36 mesh for high-*Re* models (both covering one half of the symmetric wing). The latter grid was generated by amalgamating cells close to the wall to form a "wall-function" layer.

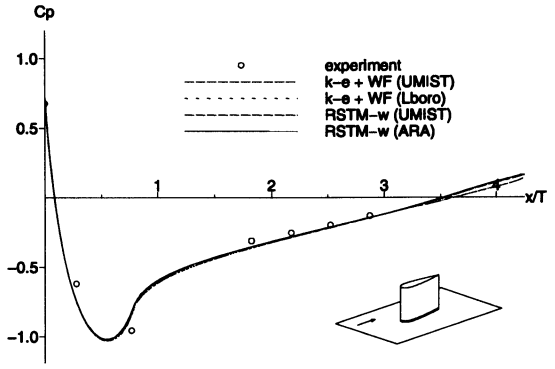

Figure 2: Pressure coefficient along the wing surface.

4 RESULTS

Comparisons between numerical solutions and experimental data were undertaken for the pressure around the wing and on the plane surface, streamwise velocity in the upstream symmetry plane, transverse velocity in cross-flow planes, and streamwise normal stress and the shear stress in cross-flow planes. Space constraints permit only a few representative results to be included. The objective here is to convey a general impression of the study and to provide representative results which justify major conclusions.

Comparisons of pressure distributions around the wing surface, from leading to trailing edge, at a position just above the plane wall, are given in Figure 2. These distributions illustrate, first, that the pressure is, as expected, fairly insensitive to turbulence modelling; and second, that the solutions arising from different partner codes are very close. The pressure is dictated, principally, by the inviscid mechanisms associated with the wing profile displacing the oncoming flow. As the adverse pressure gradient in the streamwise direction is mild (except in the wing-nose region), the boundary layer on the wing is thin and well described by any well-calibrated turbulence model. The horse-shoe vortex, whilst being a consequence of viscous mechanisms, is embedded within the streamwise flow, the gross structure of which is only mildly affected by the vortex and by turbulence transport. The pressure contours on the plane wall (not included) do reveal, however, some sensitivity to turbulence modelling, especially close to the wing's leading edge. It is in this region that the horseshoe vortex forms and where the separated flow, which *is* highly sensitive to modelling, affects most strongly the pressure field.

A feature which *is* manifestly sensitive to turbulence modelling is the recirculation zone just ahead of the wing leading edge. This is demonstrated in Figure 3 which shows velocity-vector fields in the plane bisecting the wing. The experimental field is

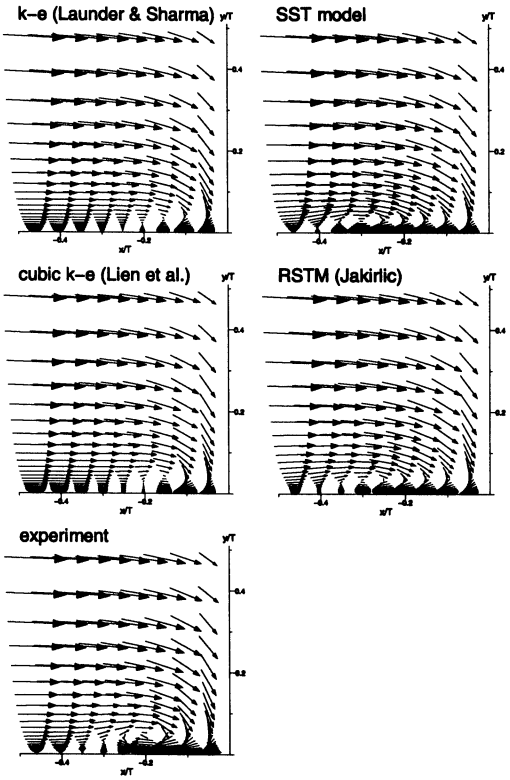

Figure 3: Velocity vectors on upwind symmetry plane.

characterised by a fairly thick vortex extending upstream to about 35% of the maximum wing-profile thickness. Although, in reality, this region contains at least two additional minor vortices which are unsteady, the time-averaged field is clearly wholly dominated by a single vortex. Neither the linear nor the cubic k-ε model resolves the vortex structure well, both predicting separation at around 25% and under-estimating the intensity of the reverse flow. In contrast, second-moment closure yields a much greater sensitivity of the oncoming boundary layer to the adverse pressure gradient at the wing leading edge, resulting in early separation and more intense recirculation. Much as expected, in the light of previous experience with 2D separated flows, the SST model also gives this increasing sensitivity, but this is due to a careful tuning of this model specifically for separated boundary layers (one facet of which is discussed later) and the use of the ω-equation in the near-wall region, which is known to give a substantially higher sensitivity to adverse pressure gradient than the ε-equation.

Figure 4 shows contours of the streamwise normal stress in the upstream symmetry plane (same as Figure 3). These contours are highly sensitive indicators of the structure of the upstream vortex and also identify its strength in terms of the turbulence-generating strain within it. The contours indicate, here again, the predictive benefits arising from second-moment closure. Only this model is able to return, with any degree of realism, the significant elevation of the streamwise normal stress, through

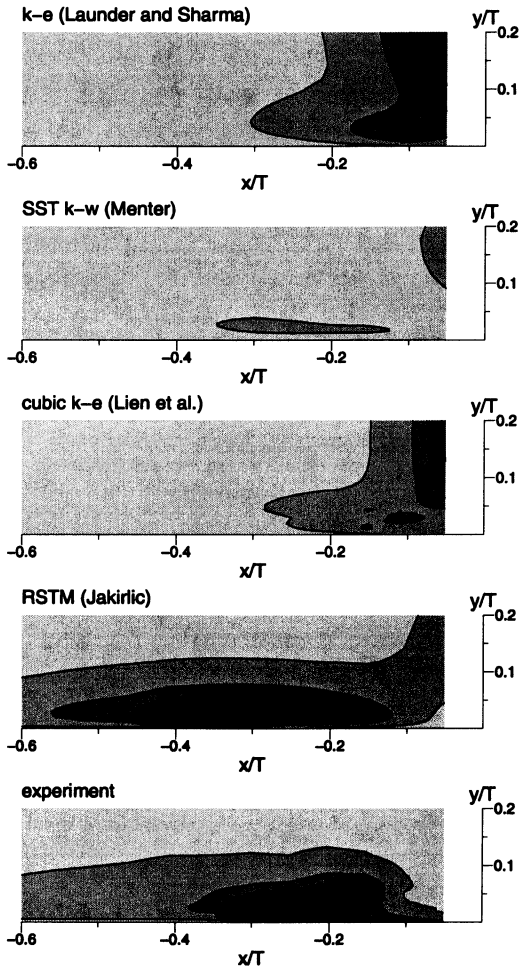

Figure 4: Streamwise normal stress in upwind symmetry plane.

shear-induced generation, in the intensely sheared central portion of the vortex. In effect, this is one of a number of facets reflecting the ability of the model to resolve normal-stress anisotropy and its interaction with stress generation. The particularly low level of the normal stress predicted by the SST model is striking and indicative of the reason for the favourable mean-flow behaviour it returns in Figure 3. Along with low streamwise normal stress, the model also predicts a low level of turbulence energy (not included). Because the model includes a direct relationship between the shear stress and the turbulence energy, the result is a reduced shear-stress level and hence an enlarged recirculation zone. While this linkage is phenomenologically advantageous, it reflects a wrong representation of the real physical interactions. In reality, the shear stress in the recirculation zone is driven, principally, by the interaction between the wall-normal turbulence intensity and the shear strain. This interaction and the low rate of stress generation associated with normal straining on either side of the separation point, result in relatively low shear stress levels in the vicinity of the separation point, thus delaying the onset of separation. The shear-stress contours (not included) returned by the Reynolds-

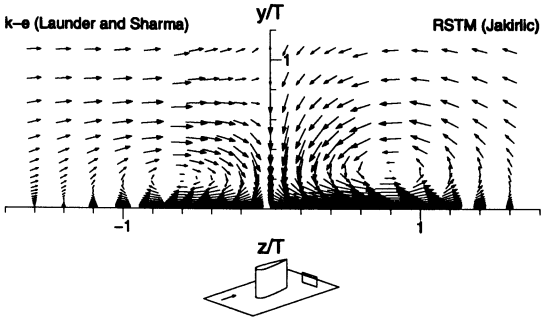

Figure 5: Transverse motion in a cross-stream plane.

stress model suggest that the above processes are represented with a fair degree of realism.

Figure 5 shows two velocity-vector fields of the transverse-flow motion structure predicted by linear k-ε and Reynolds-stress models in a cross-stream plane downstream of the trailing edge (x/T=6.38 where T is maximum wing thickness). These plots convey an impression of the significant sensitivity of the downstream structure of the horseshoe vortex to turbulence modeling. Thus, the Reynolds-stress model predicts a considerably larger vortex than that arising from the linear k-ε model, with a more pronounced transverse motion and a vortex center which is further removed from both the wing surface and the flat plate. These differences are of some importance to the results presented next in Figures 6 and 7.

Comparisons of contours of streamwise velocity just downstream of the wing (x/T=4.46) are given in Figure 6. Reference to the experimental plot reveals the presence of a fairly thin boundary layer on the wing surface and a significant thickening of the flat-plate boundary layer at the position in which the transverse vortex motion lifts boundary-layer fluid upwards towards the free stream. These features are poorly returned, especially by the linear k-ε model, but also by the cubic form and the SST variant. Only the Reynolds-stress model gives a broadly satisfactory behaviour due to the intensity of the transverse motion it predicts. This result may be claimed to reinforce the conclusion that this model returns a realistic structure of the vortex throughout its length of evolution from the wing leading edge.

The superiority of second-moment modelling is finally illustrated by Figure 7 which shows the streamwise stress at the same plane as that in Figure 6. The linear k-ε model returns large levels of stress (and turbulence energy) over most of the cross-sectional area, signifying high upstream generation (see Figure 4) and downstream advection of turbulence. Only the Reynolds-stress model returns a field which contains the 'foot-print' of the vortex, specifically the rotational advection of energy generated in the junction and along the walls. Again, the SST model comes closest to the Reynolds-stress

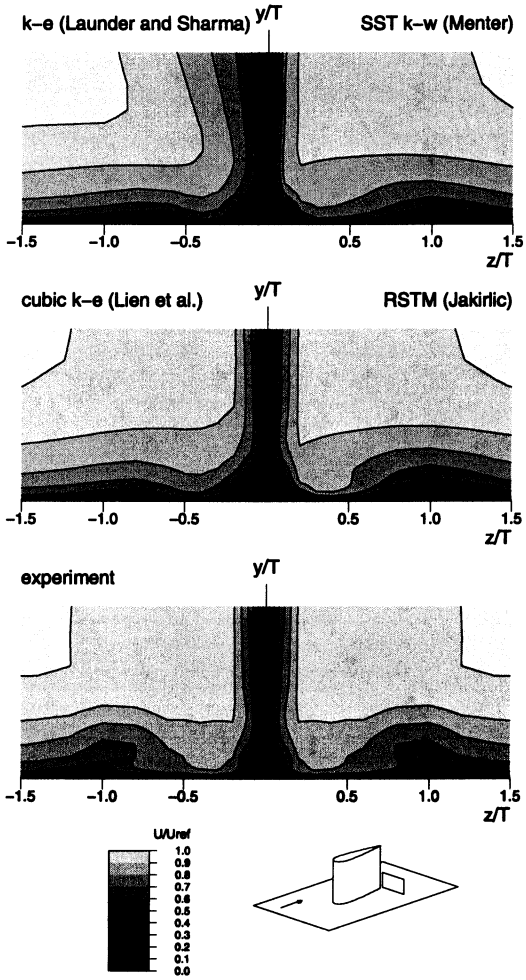

Figure 6: Streamwise mean-velocity contours.

model, but the level of agreement with experiment is significantly poorer.

5. CONCLUDING REMARKS

The main elements of a collaborative computational study of turbulence-model performance in a wing/body-junction flow have been presented. While the study is not (and cannot be) exhaustive, in terms of either model coverage or partner/model overlap, it has provided valuable information on the relative performance of some of the most widely-used models in CFD for Aero/Mechanical Engineering applications. The fact that several partners interacted closely in respect of numerical accuracy, code-dependence, grid and boundary conditions deserves to be highlighted for it provides added confidence in the solutions.

The study provides strong evidence that, at least for this type of 3D flow, second-moment closure performs well and is superior to other models. The only model which came close to second-moment closure is the SST model which has been carefully crafted and calibrated to respond sensitively to adverse pressure gradient provoking separation. If anything, this sensitivity appears to be too strong,

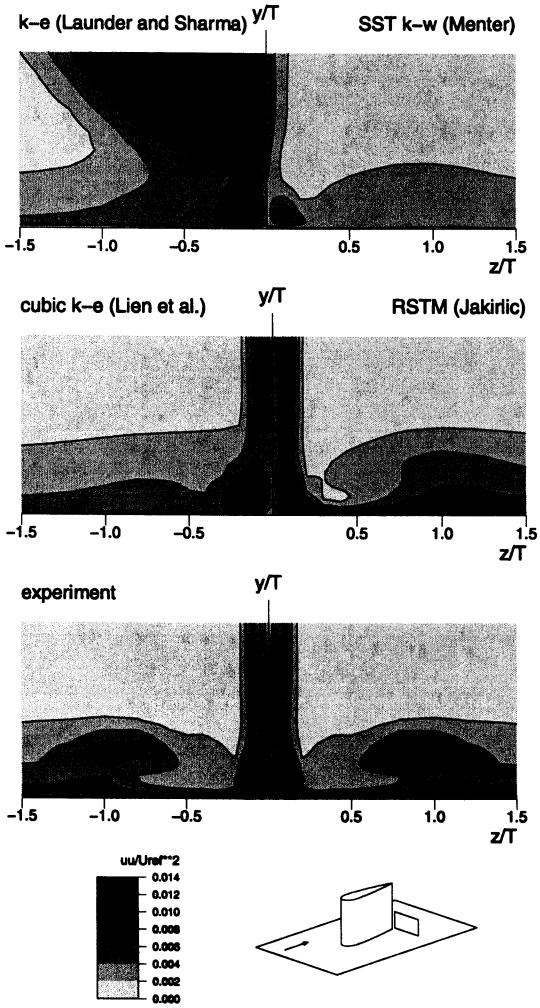

Figure 7: Streamwise normal stress.

and this is consistent with conclusions derived from other studies directed at compressible separated flows. Somewhat disappointingly, both cubic eddy-viscosity models, of which only one has been considered herein, did not perform much better than the linear forms, and this is at variance with the outcome of studies directed at 2D separated flows, both incompressible and compressible, in which such models gave results comparable with second-moment closure.

Acknowledgements

The authors are grateful to EPSRC, BAE Systems, DERA and RR plc for their financial support, and to ARA for allowing their solutions to be included.

References

Apsley, D.D., Chen, W.-L. and Leschziner, M.A., 1998, *J. Hydraulic Research*, Vol. 35, pp. 723-748.

Apsley, D.D. and Leschziner, M.A., 1998, *Int. J. Heat Fluid Flow*, Vol. 19, pp. 209-222.

Baker, C.J., 1985, *J. Wind Engrg. Indust. Aerodyn.*, Vol. 18, pp. 263-274.

Chen, H.-C., 1995, *J. Fluids Engrg*, Vol. 117, pp. 557-563.

Craft, T.J., Launder, B.E. and Suga, 1996, *Int. J. Heat Fluid Flow*, Vol. 17, pp. 108-115.

Devenport, W.J. and Simpson, R.L., 1990, *J. Fluid Mech*, Vol. 210, pp. 23-55.

Fleming, J.L., Simpson, R.L. and Devenport, W.J., 1993, *Experiments in Fluids*, Vol. 14, pp. 366-378.

Fu, S., Zhai, Z., Rung, T. and Thiele, F., 1997, "Numerical study of flow past a wing-body junction with a realisable nonlinear EVM", *Proc. 11th Symp. Turbulent Shear Flows*, Grenoble, pp. 6.7-6.12.

Gibson, M.M. and Launder, B.E., 1978, *J. Fluid Mech.*, Vol. 86, pp. 491-511.

Jakirlic, S. and Hanjalic, K., 1995, "A second moment closure for non-equilibrium and separating high and low-Re number flows", *Proc. 10th Symp. on Turbulent shear Flows*, Pennsylvania State University, pp. 23.25-23.30.

Kalitzin, G., Gould, A.R.B and Benton, J.J., 1996, "Application of two-equation turbulence models in aircraft design", AIAA paper 96-0327.

Launder, B.E. and Sharma, B.I., 1974, *Letters in Heat and Mass Transfer*, Vol. 1, pp. 131-138.

Launder, B.E. and Spalding, D.B., 1974, *Comput. Methods Appl. Mech. Engrg*, Vol. 3, pp. 269-289.

Lien, F.-S., Chen, W.-L. and Leschziner, M.A, 1996, "Low-Reynolds-number eddy-viscosity modelling based on non-linear stress-strain/vorticity relations", *Engineering Turbulence Modelling and Experiments 3*, (W.Rodi and G. Bergeles, Eds.), Elsevier, pp. 91-100.

Lien, F.S. and Leschziner, M.A., 1993, *J. Fluids Engrg.*, Vol. 115, pp. 717-725.

Menter, F.R., 1994, *J. AIAA*, Vol. 32, pp. 1598-1605.

Parneix, S., Durbin, P.A. and Behnia, M., 1998, *Flow, Turbulence and Combustion*, Vol. 60, 19-46.

Rodi, W., Bonnin, J.-C. and Buchal, T., 1995, *Proc. of 4th ERCOFTAC/IAHR Workshop on Refined Flow Modelling*, University of Karlsruhe.

Shabaka, I.M.M.A. and Bradshaw, P., 1981, *J. AIAA*, Vol. 19, pp. 131-132.

Shih, T-H., Zhu, J. and Lumley, J.L., 1995, *Comput. Methods Appl. Mech. Engrg.*, Vol. 125, pp. 287-302.

Speziale, C.G., Sarkar, S. and Gatski, T.B., 1991, *J. Fluid Mech*, Vol. 227, 245-272.

Wilcox, D.C., 1988, *J. AIAA*, Vol. 26, pp. 1299-1310.

Wilcox, D.C., 1988, *J. AIAA*, Vol. 26, pp. 1311-1320.